JCI The Journal of Clinical Investigation

Muscle-specific expression of IGF-1 blocks angiotensin II–induced skeletal muscle wasting

Yao-Hua Song, … , Nadia Rosenthal, Patrick Delafontaine

J Clin Invest. 2005;115(2):451-458. https://doi.org/10.1172/JCI22324.

Article **Cardiology**

Advanced congestive heart failure is associated with activation of the renin-angiotensin system and skeletal muscle wasting. We previously showed that angiotensin II infusion in rats produces cachexia secondarily to increased muscle proteolysis and also decreases levels of circulating and skeletal muscle IGF-1. Here we show that angiotensin II markedly downregulates phospho-Akt and activates caspase-3 in skeletal muscle, leading to actin cleavage, an important component of muscle proteolysis, and to increased apoptosis. These changes are blocked by muscle-specific expression of IGF-1, likely via the Akt/mTOR/p70S6K signaling pathway. We also demonstrate that mRNA levels of the ubiquitin ligases atrogin-1 and muscle ring finger–1 are upregulated in angiotensin II–infused WT, but not in IGF-1–transgenic, mice. These findings strongly suggest that angiotensin II downregulation of IGF-1 in skeletal muscle is causally related to angiotensin II–induced wasting. Because the renin-angiotensin system is activated in many catabolic conditions, our findings have broad implications for understanding mechanisms of skeletal muscle wasting and provide a rationale for new therapeutic approaches.

Muscle-specific expression of IGF-1 blocks angiotensin II–induced skeletal muscle wasting

Yao-Hua Song,[1] Yangxin Li,[1] Jie Du,[2] William E. Mitch,[2] Nadia Rosenthal,[3] and Patrick Delafontaine[1]

[1]Tulane University Health Sciences Center, New Orleans, Louisiana, USA. [2]University of Texas Medical Branch, Galveston, Texas, USA. [3]European Molecular Biology Laboratory Mouse Biology Program, Rome, Italy.

Advanced congestive heart failure is associated with activation of the renin-angiotensin system and skeletal muscle wasting. We previously showed that angiotensin II infusion in rats produces cachexia secondarily to increased muscle proteolysis and also decreases levels of circulating and skeletal muscle IGF-1. Here we show that angiotensin II markedly downregulates phospho-Akt and activates caspase-3 in skeletal muscle, leading to actin cleavage, an important component of muscle proteolysis, and to increased apoptosis. These changes are blocked by muscle-specific expression of IGF-1, likely via the Akt/mTOR/p70S6K signaling pathway. We also demonstrate that mRNA levels of the ubiquitin ligases atrogin-1 and muscle ring finger–1 are upregulated in angiotensin II–infused WT, but not in IGF-1–transgenic, mice. These findings strongly suggest that angiotensin II downregulation of IGF-1 in skeletal muscle is causally related to angiotensin II–induced wasting. Because the renin-angiotensin system is activated in many catabolic conditions, our findings have broad implications for understanding mechanisms of skeletal muscle wasting and provide a rationale for new therapeutic approaches.

Introduction

Congestive heart failure (CHF) is a leading cause of cardiovascular mortality and morbidity (1). CHF is associated with elevated circulating levels of angiotensin II (2) and muscle wasting, which is an important predictor of poor outcome in patients with this disease (3, 4).

We have recently demonstrated that angiotensin II infusion in the rat produced a marked reduction in body weight accompanied by depression of circulating and skeletal muscle IGF-1 (5). These findings suggested that downregulation of IGF-1 signaling in skeletal muscle could mediate the wasting effect of angiotensin II. Recent studies using in vitro models of muscle atrophy have indicated that IGF-1 acts through Akt and Foxo to suppress atrogin-1/muscle ring finger–1 (atrogin-1/MuRF-1) transcription (6). Atrogin-1 and MuRF-1 are ubiquitin ligases whose expression is elevated in various muscle atrophy models (7). In vivo studies have indicated that apoptosis is also involved in muscle wasting (8, 9). Furthermore, we have recently shown that activation of caspase-3 leading to actin cleavage contributes to proteolysis in catabolic conditions such as uremia or diabetes and leaves a characteristic 14-kDa actin fragment in muscle (10). In view of the potent anabolic and antiapoptotic effects of IGF-1 (11, 12), we hypothesized that downregulation of IGF-1 signaling in response to angiotensin II would lead to a coordinated activation of both caspase-3–mediated apoptosis and activation of the ubiquitin-proteasome (Ub-P'some) pathway, resulting in loss of skeletal muscle. We used skeletal muscle–specific IGF-1–transgenic mice to identify the downstream signal pathways involved in angiotensin II–induced muscle wasting. We demonstrate that angiotensin II downregulation of IGF-1 signaling via the Akt/mTOR/p70S6K pathway is a critical step that leads to caspase-3 activation, actin cleavage, stimulation of ubiquitinization, and increased apoptosis. Targeting the IGF-1 pathway in catabolic conditions, particularly those in which the renin-angiotensin system is activated, will likely provide therapeutic benefit.

Results

Angiotensin II–induced protein degradation in vivo involves activation of caspase-3 and actin cleavage. We infused 12- to 16-week-old C57BL/6 mice with 500 ng/kg/min angiotensin II or vehicle (n = 6 per group) for 7 days, and sham-infused mice were pair fed. Angiotensin II infusion increased blood pressure (Figure 1A) and reduced body weight (Figure 1B), which was similar to our previous findings in rats. Gastrocnemius and soleus muscle from angiotensin II–infused mice at 7 days weighed less than those from pair-fed, sham-infused controls (Figure 1, C and D). We have recently shown that actomyosin cleavage by recombinant caspase-3 increases proteolysis via the Ub-P'some system. We found a 6-fold increase in caspase-3 activity in gastrocnemius muscle ($P < 0.01$) after 7 days of angiotensin II infusion (Figure 2A). Activation of caspase-3 requires proteolytic processing of its inactive zymogen into active p17 and p12 subunits. We detected significant accumulation of cleaved p17 subunit of caspase-3 in the muscle of angiotensin II–infused mice (Figure 2B). Furthermore, angiotensin II infusion markedly increased levels of the characteristic footprint of caspase-3 activation, a 14-kDa actin fragment (Figure 2C), and this increase was blunted by the cell-permeable caspase inhibitor DEVD-CHO (Figure 2D), which indicates that caspase-3 activation was responsible for the accumulation of cleaved actin fragment in muscles of angiotensin II–infused animals. We have previously shown that accumulation of cleaved actin is associated with proteolysis

Nonstandard abbreviations used: CHF, congestive heart failure; EDL, extensor digitorum longus; GSK3β; glycogen synthase kinase 3β; IRS-1, insulin receptor substrate–1; LAD, left anterior descending coronary artery; MLC, myosin light chain; mTOR, mallalian target of rapamycin; MuRF-1; muscle ring finger–1; Ub-P'some, ubiquitin-proteasome.

Conflict of interest: The authors have declared that no conflict of interest exists.

Citation for this article: *J. Clin. Invest.* **115**:451–458 (2005). doi:10.1172/JCI200522324.

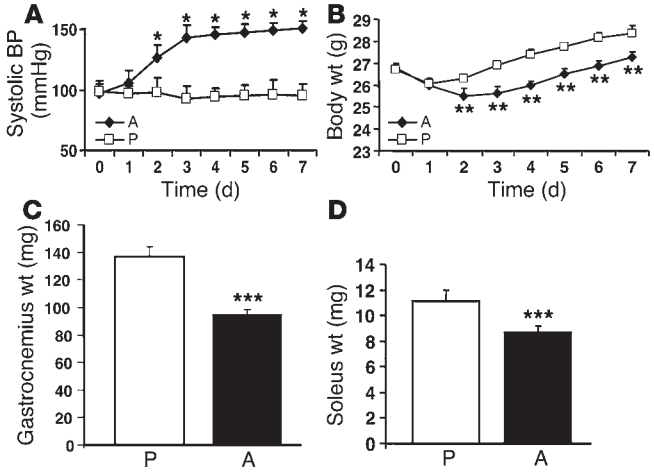

Figure 1
Angiotensin II produces muscle wasting in mice. C57BL/6 mice were either angiotensin II infused or sham infused and pair fed. Angiotensin II (**A**) markedly increased blood pressure (*P < 0.001, angiotensin II–infused vs. pair-fed), (**B**) produced relative weight loss (**P < 0.01 angiotensin II–infused vs. pair-fed), and (**C** and **D**) reduced muscle mass (***P < 0.05, angiotensin II–infused vs. pair-fed). A, angiotensin II–infused; P, pair-fed.

through the Ub-P'some system (10). Evidence for involvement of the Ub-P'some system in animal models of catabolic conditions includes increased mRNA levels of the ubiquitin ligases atrogin-1/muscle atrophy F-box (atrogin-1/MAFbx) and MuRF-1 (7, 13). Using real-time PCR we found that angiotensin II caused a 24-fold and a 5-fold increase of atrogin-1 and MuRF-1 mRNA levels, respectively (Supplemental Figure 1; supplemental material available online with this article, doi:10.1172/JCI200522324DS1). Furthermore, there was a marked increase in ubiquitinated proteins in muscle from angiotensin II–infused mice (Figure 2E). Since there are a number of reports suggesting that the calpain/calpastatin system (14–16) is important in muscle wasting, we measured calpain activity in our model using gastrocnemius muscle lysates from angiotensin II–infused and pair-fed mice. Our data showed that there was no significant difference in calpain activity between angiotensin II and pair-fed animals. Furthermore, DEVD-CHO had no effect on calpain activity (Supplemental Figure 2). Thus, angiotensin II–induced muscle loss involves activation of caspase-3, actin cleavage, and activation of the Ub-P'some system.

Angiotensin II infusion in mice induces serine phosphorylation of insulin receptor substrate–1 and reduces Akt, GSK3β and Foxo phosphorylation in skeletal muscle. We examined the mechanisms whereby caspase-3 became activated by angiotensin II. It has been shown that diminished Akt signaling promotes the cleavage and activation of caspase-3 (17). Using anti–phospho-Akt antibody (Ser473), we found that expression of phospho-Akt, but not total Akt, was reduced by angiotensin II infusion (Figure 2F). We next investigated the upstream signals that lead to the downregulation of Akt. There have been several reports that angiotensin II can inhibit both IGF-1 and insulin-stimulated PI3K activity and Akt activation, potentially via serine phosphorylation of insulin receptor substrate–1 (IRS-1) (18–20). We found that angiotensin II markedly stimulated Ser307 phosphorylation of IRS-1, which was not detected in muscle from control mice (Figure 2G).

Downstream effectors of Akt that can mediate hypertrophy include the negative regulator glycogen synthase kinase 3β (GSK3β; phosphorylated and inactivated by Akt) and positive regulators mammalian target of rapamycin (mTOR) and p70S6K. Additionally, the forkhead transcription factor Foxo1 is phosphorylated and inactivated by insulin and IGF-1 through an Akt-dependent mechanism, and this phosphorylation has

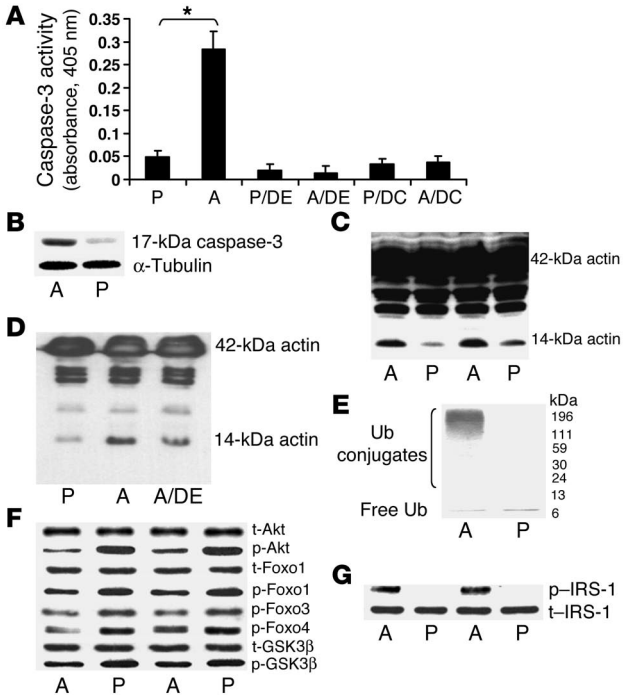

Figure 2
Angiotensin II decreases Akt phosphorylation and activates caspase-3, producing actin cleavage and increased protein ubiquitinization in skeletal muscle. Mice were either angiotensin II infused or sham infused and pair fed (n = 5 per group, 7 days) and gastrocnemius lysates assessed for (**A**) caspase-3 activity (*P < 0.01 angiotensin II– vs. sham-infused); (**B**) levels of activated (17-kDa) caspase-3 by Western blotting; (**C**) actin cleavage as determined by accumulation of 14-kDa actin fragment; (**D**) accumulation of 14-kDa actin fragment with or without caspase-3 inhibitor DEVD-CHO; (**E**) expression of proteins conjugated to ubiquitin (Ub); (**F**) expression levels of phospho–Akt (p-Akt), total Akt (t-Akt), phospho- and total Foxos, and phospho-GSK3β and total GSK3β; and (**G**) Ser307 phosphorylation of IRS-1 after immunoprecipitation with anti–IRS-1 antibody and SDS-PAGE and Western blotting. A/DE and P/DE, angiotensin II–infused and pair-fed with caspase-3 inhibitor DEVD-CHO, which was added to muscle lysates; A/DC and P/DC, angiotensin II–infused and pair-fed with caspase inhibitor Z-Asp-2,6-dichlorobenzoyloxymethylketone, which was administered to mice for 7 days.

been shown to be critical for insulin/IGF-1 antiapoptotic effects, potentially through a caspase-3–dependent mechanism (21). Furthermore, it has been shown that IGF-1 and insulin inhibit the expression of atrogin-1/MuRF-1 by inactivating Foxos (6). We found that angiotensin II infusion reduced phosphorylation of Foxo1, Foxo3, Foxo4, and GSK3β (Figure 2F).

To demonstrate that caspase-3 activation is required in angiotensin II–induced muscle wasting, we administered a caspase inhibitor Z-Asp-2,6-dichlorobenzoyloxymethylketone to mice. This inhibitor has been shown to inhibit caspase-3 activation and ameliorate apoptosis and cardiac remodeling in rats with myocardial infarction (22). Our data showed that the caspase inhibitor markedly blunted the wasting effect of angiotensin II. Thus, there was no statistically significant difference in body and muscle weight between angiotensin II–infused and pair-fed groups treated with caspase inhibitor after 5 days (Supplemental Figure 3, A–D). We further analyzed caspase-3 activity, actin cleavage, and protein ubiquitinization in mice receiving the caspase inhibitor. As shown in Figure 2A, caspase-3 activity was completely inhibited both in sham-infused, pair-fed and in angiotensin II–infused groups, and no actin cleavage was detected (Supplemental Figure 3E). Ubiquitinization was also minimal, and there was no difference between angiotensin II and pair-fed groups (Supplemental Figure 3F). Therefore, our data suggest that caspase-3 activation is required for actin cleavage and for increased protein ubiquitinization. Our data show that the expression levels of both atrogin-1 and MuRF-1, measured by real-time PCR, remain elevated in the angiotensin II–group compared with the pair-fed group (Supplemental Figure 1). However, the degree of angiotensin II induction of atrogin-1/MuRF-1 expression was blunted in the presence of caspase-3 inhibition. Thus, the angiotensin II–induced fold increases in atrogin-1 and MuRF-1 were 12.2 ± 1.2 and 1.4 ± 0.3, respectively, with caspase inhibition, as opposed to 24 ± 0.5 and 5 ± 0.3 without caspase inhibition. This finding suggests that angiotensin upregulation of ubiquitin ligases is in part caspase-3 dependent.

Angiotensin II–induced muscle wasting is not due to reduced potassium levels and is glucocorticoid dependent. It is possible that angiotensin II infusion, by raising aldosterone levels, could produce hypokalemia and tissue potassium depletion, which could contribute to muscle wasting. We thus measured circulating plasma K^+ levels in angiotensin II–infused and pair-fed mice at day 7 ($n = 5$ per group) and did not find a significant difference (pair-fed, 4.01 ± 0.14 mM; angiotensin II–infused, 4.07 ± 0.22 mM; $P = 0.59$). Because K^+ serum homeostasis tends to be maintained at the expense of the intracellular compartment, measuring serum levels may not be adequate; therefore, we also measured muscle K^+ content. However, we did not find a difference in gastrocnemius muscle K^+ content (pair-fed, 104.9 ± 1.3 μmol/g wet weight; angiotensin II–infused, 105.5 ± 1.6 μmol/g wet weight; $n = 5$, $P = 0.53$).

The muscle-wasting effect of angiotensin II could be mediated via a direct interaction between angiotensin II and its receptors on skeletal muscle tissue; however, muscle angiotensin II receptor expression decreases at the end of gestation to very low levels in differentiated muscle (23, 24). Alternatively, the angiotensin II–induced decrease in IGF-1 and muscle loss could be mediated by intermediate factors that are regulated by angiotensin II, such as glucocorticoids. Indeed, we have shown previously that there is an increase in urinary corticosterone levels with angiotensin II infusion in rats (25). It has been shown that catabolic doses of glucocorticoids injected in the rat activate the ubiquitin pathway of protein degradation (26) and reduce skeletal muscle expression of IGF-1 (27). We also found that glucocorticoids are necessary for activation of the Ub-P'some system in acidosis or diabetes (28–30). We tested an inhibitor of glucocorticoids, RU486 (2 mg/kg/d, a dose shown to be effective in mice; ref. 31), and found that it blunted the angiotensin II–induced relative weight loss and reduction in muscle mass (Figure 3, A–C).

Targeted expression of IGF-1 transgene in skeletal muscle completely inhibits angiotensin II–induced weight loss and muscle wasting. We have recently demonstrated that angiotensin II–induced muscle wasting is associated with a reduction in circulating and skeletal muscle levels of IGF-1; however, systemic administration of IGF-1 with angiotensin II did not prevent muscle wasting in rats, which suggests that the autocrine IGF-1 system was involved (25). In our present study, we found that angiotensin II infusion reduced muscle IGF-1 mRNA levels (measured by real-time PCR) by 37% ± 6% at 7 days ($P < 0.05$, angiotensin II–infused vs. pair-fed mice). To determine whether IGF-1 overexpression in muscle could prevent angiotensin II–induced wasting, we used *MLC/mIgf-1* mice, which express a local IGF-1 isoform in muscle under control of the myosin light chain (MLC) promoter (32).

We infused WT (FVB) mice or transgenic *MLC/mIgf-1* mice with angiotensin II and sham-infused pair-fed mice for 7 days. The hypertensive response to angiotensin II at 7 days was virtually identical in transgenic and WT mice (58 ± 6.7 mmHg increase vs. 54.8 ± 12.1 mmHg increase, respectively), and the baseline blood pressure was the same in both groups. The angiotensin II–induced relative weight loss in WT mice (Figure 4A) was completely prevented in *MLC/mIgf-1* transgenics (Figure 4B), as was the reduction in gastrocnemius and extensor digitorum longus

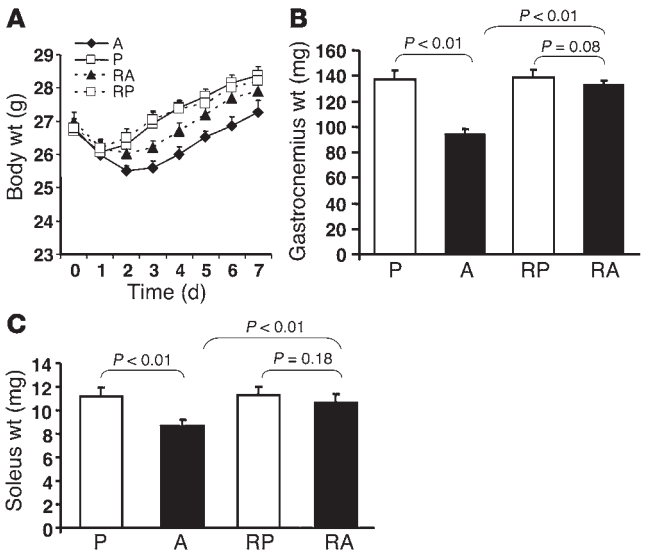

Figure 3
Angiotensin II–induced muscle wasting in mice is in part glucocorticoid dependent. Mice were either angiotensin II infused or sham infused with daily injections of RU486 or vehicle and pair fed. RU486 significantly inhibited the angiotensin II–induced (**A**) relative loss of body weight ($P < 0.01$, angiotensin II–infused with RU486 [RA] vs. angiotensin II–infused), and (**B** and **C**) decrease in muscle mass as assessed at 7 days. RP, pair-fed with RU486.

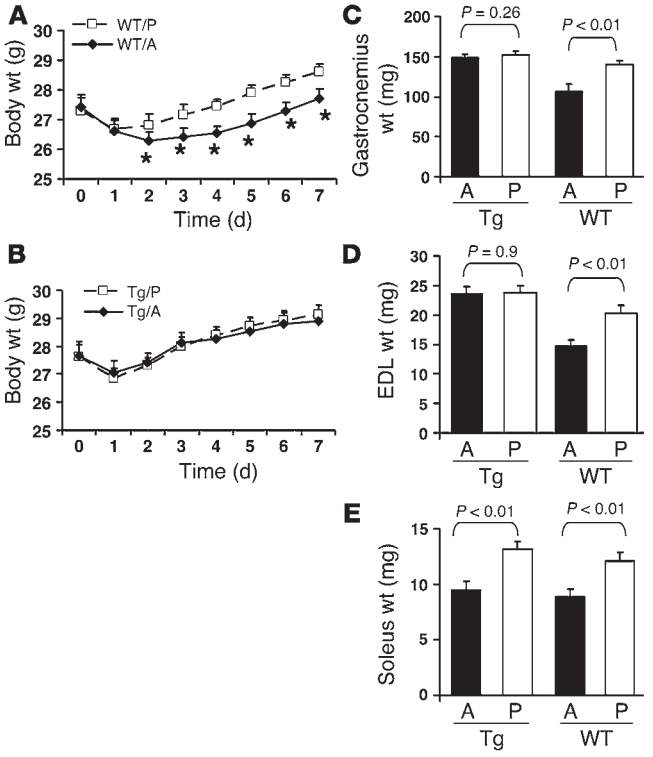

Figure 4
Skeletal muscle–specific expression of an IGF-1 transgene blocks angiotensin II–induced wasting. WT or transgenic (Tg) mice were either angiotensin II infused or sham infused and pair fed for 7 days, and daily weights were measured (**A** and **B**) and muscle weights obtained at 7 days (**C**–**E**). The relative weight loss in angiotensin II–infused WT mice (**A**; **P* < 0.01 WT/angiotensin II–infused vs. WT/pair-fed) was blocked in transgenic mice (**B**) with preferential fast-fiber effect (**C** and **D**).

(EDL) muscle weight (Figure 4, C and D). However, soleus muscle weight was reduced in response to angiotensin II infusion in both WT and transgenic mice (Figure 4E), consistent with the preferential expression of IGF-1 in fast fibers. We then tested whether IGF-1 overexpression suppressed angiotensin II induction of ubiquitin ligases. In contrast to what was found in the WT FVB mice, angiotensin II infusion did not increase expression of atrogin-1 and MuRF-1 in the gastrocnemius muscle of the *MLC/mIgf-1* mice (Supplemental Figure 1). Indeed, in transgenic mice, angiotensin II infusion caused a small decrease in atrogin-1 (fold decrease of 0.65 ± 0.08, angiotensin II–infused vs. pair-fed; $P < 0.05$) and MuRF-1 (fold decrease of 0.62 ± 0.05, angiotensin II–infused vs. pair-fed; $P < 0.01$) mRNA levels.

We next examined the signal pathways that mediate IGF-1's anabolic effect in the *MLC/mIgf-1* mice. IGF-1 induces muscle hypertrophy by activating the type 1 IGF-1 receptor (IGF-1R), which then activates multiple signaling pathways, including the PI3K and MAPK pathways. There were no significant differences in IGF-1R, phospho- or total Akt, and phospho- or total MAPK between *MLC/mIgf-1* transgenic and WT mice at basal levels (Figure 5A). However, the expression level of phospho-mTOR and phospho-p70S6K was increased at basal levels in the *MLC/mIgf-1* mice (Figure 5B). Furthermore, phospho-mTOR and phospho-p70S6K levels were reduced in angiotensin II–infused WT but maintained in the angiotensin II–infused *MLC/mIgf-1* mice (Figure 5B). The angiotensin II–induced reduction in Akt phosphorylation that occurred in WT mice was completely blocked in the *MLC/mIgf-1* mice (Figure 5C). Consequently, caspase-3 activation (Figure 5C) and actin cleavage (Figure 5D) were prevented in the angiotensin II–infused *MLC/mIgf-1* mice. These data demonstrate that the Akt/mTOR/p70S6K pathway remains active in the *MLC/mIgf-1* mice receiving angiotensin II.

In order to provide additional evidence of the role of the Akt/mTOR/p70S6K pathway in skeletal muscle wasting, we studied a rat ischemic cardiomyopathy model. Heart failure was induced by left anterior descending coronary artery (LAD) ligation, and muscles were harvested at 2 weeks. The rats with LAD ligation had reduced gastrocnemius (LAD-ligated, 1.5 ± 0.08 g; sham-operated 1.7 ± 0.1 g; $P < 0.05$) as well as soleus muscle mass (LAD-ligated, 122.8 ± 8.7 mg; sham, 152.4 ± 9.3 mg; $P < 0.01$). Western blotting showed that the levels of phospho-Akt and phospho-p70S6K were markedly reduced in gastrocnemius muscle from LAD-ligated rats compared with those from sham-operated rats. The levels of total Akt and total p70S6K were not different between LAD-ligated and sham-operated rats (Supplemental Figure 4).

Angiotensin II induces apoptosis of skeletal muscle, which is prevented by autocrine IGF-1. The activation of caspase-3 in our angiotensin II–infused animals prompted us to investigate whether apoptosis is

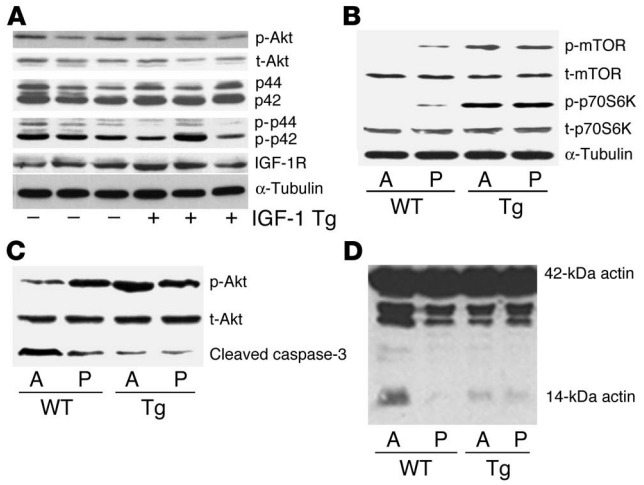

Figure 5
Involvement of Akt/mTOR/p70S6K kinases in the ability of the *MLC/mIgf-1* transgene to prevent angiotensin II–induced muscle loss. (**A**) Basal characterization of signaling pathways in *MLC/mIgf-1* mice. Gastrocnemius lysates from WT or *MLC/mIgf-1* mice were subjected to SDS-PAGE and Western blotting with indicated antibodies. There is no significant difference in baseline levels of IGF-1 receptor (IGF-1R), phospho- or total Akt, and phospho- or total MAPK in transgenics. (**B**) Phospho-mTOR and phospho-p70S6K expression was diminished in muscles of angiotensin II–infused WT mice compared with pair-fed controls but was maintained in the angiotensin II–infused *MLC/mIgf-1* mice. Additionally, expression of phospho-mTOR and phospho-p70S6K was increased at basal levels in transgenic mice compared with WT. (**C**) Phospho-Akt expression was maintained in angiotensin II–infused *MLC/mIgf-1* mice, accompanied by diminished caspase-3 cleavage. (**D**) The accumulation of 14-kDa actin fragment was significantly reduced in the angiotensin II–infused *MLC/mIgf-1* mice compared with WT mice.

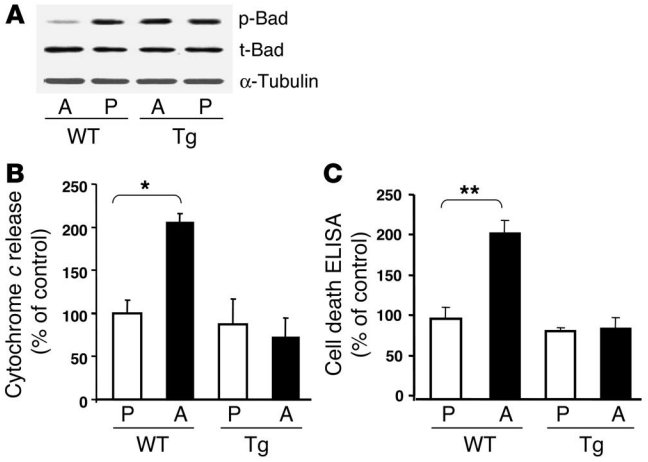

Figure 6

Angiotensin II–induced muscle loss in WT mice is associated with (**A**) reduced levels of phospho-Bad in gastrocnemius muscle; (**B**) increased cytochrome *c* release into the cytosolic fraction (**P* < 0.05, angiotensin II–infused vs. pair-fed WT); and (**C**) DNA fragmentation as detected by cell death ELISA (***P* < 0.01, angiotensin II–infused vs. pair-fed WT). These changes were completely blunted in the transgenic mice (**A**–**C**).

involved in angiotensin II–induced muscle loss. Upstream components of the apoptosis cascade include Bad and cytochrome *c*. Akt has been shown to promote cell survival in part via its ability to phosphorylate Bad at Ser136 (33, 34). Phospho-Bad (Ser136) expression was reduced in the muscle of WT angiotensin II–infused mice compared with the pair-fed controls (Figure 6A). However, the phosphorylation of Bad was maintained in the *MLC/mIgf-1* mice infused with angiotensin II. Furthermore, there was a significant increase in cytosolic cytochrome *c* release (Figure 6B) and DNA fragmentation (Figure 6C) in response to angiotensin II in WT mice compared with the pair-fed controls, whereas these increases were prevented in the *MLC/mIgf-1* mice. TUNEL staining of gastrocnemius muscle sections showed that there was a significant increase in the number of TUNEL-positive nuclei, which was 21% ± 4% in angiotensin II–infused mice as opposed to 5% ± 2% in the pair-fed mice ($P < 0.01$) (Supplemental Figure 5).

Discussion

We have previously shown that angiotensin II–induced muscle loss was accompanied by depression of circulating and skeletal muscle IGF-1. We now demonstrate that overexpression of IGF-1 in skeletal muscle effectively blocks angiotensin II–induced muscle loss, which strongly suggests that depression of skeletal muscle IGF-1 plays a causal role in angiotensin II–induced muscle loss. Indeed, we had previously failed to correct this muscle loss by infusing IGF-1. These findings are consistent with the demonstration that a liver-specific null mutation for the IGF-1 gene, which depresses circulating but not skeletal muscle IGF-1, fails to retard muscle growth (35, 36). Our data showed that angiotensin II–induced muscle loss was prevented in the gastrocnemius and EDL muscles but not in the soleus of *MLC/mIgf-1* mice. This is explained by the fact that the expression of the *MLC/mIgf-1* transgene in adult mice is restricted to skeletal muscle and predominates in muscles enriched in fast fibers, such as the triceps, EDL, and gastrocnemius. Transgene expression is reduced in slow muscles such as the soleus, where the MLC regulatory cassette is characteristically expressed at very low levels (32).

We have recently demonstrated that caspase-3 activation and resulting actin cleavage are associated with increased protein degradation via the Ub-P'some pathway (10). We now show that caspase-3 activity is markedly increased in muscle from angiotensin II–infused mice, leading to actin cleavage. Additionally, angiotensin II increases expression of ubiquitin ligases and stimulates protein ubiquitinization in skeletal muscle. These changes are prevented by expression of an IGF-1 transgene, consistent with a model wherein the depression of skeletal muscle IGF-1 and of IGF-1 signaling plays the central role, leading to activation of caspase-3 and to increased transcription of ubiquitin ligases and increased proteolysis. We show that in addition to stimulating the Ub-P'some pathway, angiotensin II stimulates apoptosis of skeletal muscle via a reduction in Bad phosphorylation and an increase in cytosolic cytochrome *c* release. These changes are also reversed by transgenic expression of IGF-1 in muscle. It is of note that Sandri et al. (6) have recently shown that IGF-1 inhibits starvation and glucocorticoid-induced atrogin-1 expression and atrophy of cultured myotubes. This effect of IGF-1 was mediated by inactivation of Foxos. Our data extend these observations by strongly suggesting that the protective effect of IGF-1 against muscle atrophy is also mediated by its ability to maintain Bad phosphorylation in the setting of a catabolic stimulus, namely angiotensin II infusion.

Our data using a caspase inhibitor support the critical role of caspase activation in the wasting effect of angiotensin II. Thus, in the presence of caspase inhibition, the angiotensin II–induced loss of muscle weight was markedly blunted and not significant at days 5–7. Angiotensin II–induced actin cleavage and protein ubiquitinization were also inhibited by caspase inhibition. Interestingly, angiotensin II–induced upregulation of atrogin-1 and MuRF-1 mRNA levels was partially blunted in the presence of caspase inhibition, which suggests a possible involvement of a caspase-3–dependent mechanism in angiotensin II–mediated upregulation of ubiquitin ligase expression.

It is likely that the angiotensin II–induced increase in serine phosphorylation of IRS-1 (which has been shown to reduce PI3K activity; ref. 18) acts concurrently with the angiotensin II–induced depression of IGF-1 levels to reduce IGF-1 signaling, as evidenced by decreased phospho-Akt, phospho-GSK3β, and phospho-Foxos in muscle. It has been shown that diminished Akt signaling promotes the cleavage and activation of caspase-3 and subsequent cell atrophy or cell loss (17). The ability of IGF-1 overexpression to prevent angiotensin II–induced reduction in phospho-Akt and activation of caspase-3 (Figure 5C) strongly suggests that angiotensin II reduction in phospho-Akt signaling plays a pivotal role in the activation of caspase-3 and the subsequent signaling cascades leading to stimulation of the Ub-P'some pathway and increased apoptosis.

Although we have previously shown that angiotensin II–induced wasting is blocked by an angiotensin II type 1 (AT_1) receptor antagonist (5), the low expression of AT_1 receptor on differentiated muscle (23, 24) suggested an indirect effect of angiotensin II. Glucocorticoids have been shown to be required for stimulation of the Ub-P'some pathway in diabetes, fasting, and metabolic acidosis (28–30, 37, 38), and we have shown that angiotensin II infusion increases glucocorticoid levels (25). It has also been shown that acute treatment with corticosteroids decreases IGF-1 expression in rat skeletal muscle (27). We now show that RU486, a glucocorticoid receptor antagonist, significantly blocked the angiotensin II–induced weight loss, consistent with a role for glucocorticoids in

angiotensin II–induced muscle wasting. However, other cytokines such as TNF-α could also be involved.

IGF-1 is an important anabolic growth factor for skeletal muscle (11) and promotes myoblast proliferation and myogenic differentiation (39, 40), and IGF-1 expression is increased during compensatory hypertrophy of muscle (41). The signaling mechanisms mediating IGF-1–induced hypertrophy are incompletely understood and could include the PI3K/Akt pathway, the downstream mTOR/p70S6K or Akt/GSK3β pathways (42), or the serine/threonine protein phosphatase calcineurin, which mediates the dephosphorylation of the nuclear factor of activated T cells (NFAT) transcription factors (43). It is interesting to note that *MLC/mIgf-1* mice have muscle hypertrophy that is not accompanied by increased Akt phosphorylation; however, when these mice are crossed with mdx mice (an animal model for Duchenne muscular dystrophy), the resultant mdx:*MLC/mIgf-1* mice have improved muscle mass and function and a marked increase in Akt phosphorylation in muscle (12). Our study confirms that there is no increase in Akt phosphorylation in muscle from *MLC/mIgf-1* mice at basal levels. In addition, we show a marked increase in mTOR and p70S6K phosphorylation in muscle from *MLC/mIgf-1* mice. To our knowledge, this is the first report that IGF-1–mediated skeletal muscle hypertrophy is accompanied by increased phosphorylation of mTOR and p70S6K in vivo. Our data show that although overexpression of IGF-1 did not increase Akt phosphorylation in the unstimulated state, the reduction of phospho-Akt due to angiotensin II infusion was completely blocked in the *MLC/mIgf-1* mice. Additionally, mTOR and p70S6K phosphorylation was not reduced in transgenic mice receiving angiotensin II but was markedly reduced by angiotensin II in WT mice. These data indicate that IGF-1's ability to prevent angiotensin II–induced muscle loss is likely mediated via the Akt/mTOR/p70S6K pathway. In order to confirm the role of the Akt/mTOR/p70S6K pathway in muscle wasting, we studied muscle from rats with LAD ligation–induced heart failure and demonstrated a marked reduction in phosphorylated Akt and p70S6K in these muscles. Circulating angiotensin II levels are also elevated in this model (44).

It is of note that mTOR can be activated independently of Akt (45–47). Therefore, it is possible that in the *MLC/mIgf-1* mice, the anabolic action of IGF-1 may be mediated by both Akt-dependent and -independent pathways, which converge at the level of mTOR. The Akt-independent pathway may be more relevant to the basal hypertrophy present in the *MLC/mIgf-1* mice, whereas the Akt-dependent pathway may be more relevant in the setting of muscle damage, as occurs in the mdx mice and in the angiotensin II–infused mice. Thus mdx muscle, similar to muscle from angiotensin II–infused mice, has increased rates of apoptosis (12).

Apoptosis of myocytes can significantly contribute to the progressive loss of lean body weight in congestive heart failure (48, 49). Although weight loss is an important predictor of poor outcome in heart failure, mechanisms that lead to weight loss are poorly understood (2, 50–56). Anker and colleagues have reported multiple neurohormonal changes associated with the wasting syndrome, including increased plasma renin activity (57). We show that one putative mechanism for wasting in heart failure could be related to a decrease in muscle IGF-1 and IGF-1 signaling, and this is supported by the data from Hambrecht et al., showing that in CHF patients, muscle IGF-1 expression is considerably reduced in the presence of normal serum IGF-1 levels (50).

In summary, our present study demonstrates that angiotensin II–induced muscle wasting is mediated by reduced action of IGF-1 in skeletal muscle resulting from decreased IGF-1 expression and signaling, which lead to stimulation of the Ub-P'some pathway, activation of caspase-3, and apoptosis. These findings have important implications for understanding mechanisms of weight loss in conditions such as heart failure, in which the renin-angiotensin system is activated, and provide a strong rationale for developing therapeutic strategies to activate the skeletal muscle IGF-1 system in wasting conditions.

Methods

Antibodies. Antibodies against phospho-Akt (Ser473), phospho-Foxo1 (Ser256), phospho-Foxo4 (Ser193), phospho-GSK3β (Ser9), phospho-mTOR (Ser2448), phospho-p70S6K (Thr421/Ser424), phospho-Bad (Ser136), total Akt, total Foxo1, total GSK3β, total mTOR, total p70S6K, total Bad, and anti–cleaved caspase-3 were purchased from Cell Signaling Technology. C-terminus–specific anti-actin antibody was purchased from Sigma-Aldrich. Rabbit anti–IRS-1 antibody bound to protein A-Sepharose, anti–phospho-Foxo3 (Thr32) antibody, and anti–phospho–IRS-1 (Ser307) antibody were purchased from Upstate. Anti-ubiquitin polyclonal antibodies were obtained from Calbiochem.

Angiotensin II infusion model. All methods discussed in this section involving animals were approved by the Institutional Animal Care and Use Committee (IACUC) of Tulane University Health Sciences Center. Twelve- to 16-week-old male C57BL/6 mice (Harlan), IGF-1–transgenic mice, and WT FVB mice were used in this study. Osmotic minipumps (ALZET model 2001 or 1007D; ALZA Corp.) were implanted to infuse angiotensin II at a rate of 500 ng/kg/min or diluent (5). The body weight and food intake of each angiotensin II–infused mouse were measured daily, and a corresponding vehicle-infused control mouse was given the same amount of food as that eaten by the angiotensin II–infused mouse on the previous day (i.e., mice were pair fed). Blood pressures were measured noninvasively using the Visitech BP-2000 (Visitech Systems Inc.) as previously described (5). Seven days after implantation of the osmotic pumps, mice were anesthetized and tissues were removed, weighed, and snap-frozen in liquid nitrogen and stored at –80°C until processed. For 1 experiment, caspase inhibitor (Z-Asp-2,6-dichlorobenzoyloxymethylketone; Alexis Biochemicals) was injected intraperitoneally for 7 days (8.8 mg/g/d) (22, 58) and mice were either sham-infused (n = 5) or infused with angiotensin II (n = 5).

Myocardial infarction model. Myocardial infarction was induced by the ligation of the left coronary artery, as described previously (59). Briefly, male Sprague-Dawley rats weighing approximately 280 g each were anesthetized with ketamine (50 mg/kg i.p.) and xylazine (10 mg/kg i.p.) and tracheally ventilated with room air using a rodent ventilator (Harvard Apparatus). After a left lateral thoracotomy in the fifth intercostal space was performed, the left coronary artery was ligated. Sham-operated animals underwent a similar procedure without the actual ligation. Animals were sacrificed 2 weeks after LAD ligation and skeletal muscles collected for analysis.

Western blot. Samples were solubilized in Laemmli buffer and proteins separated by electrophoresis on 12% SDS-polyacrylamide gels. Proteins were blotted onto PVDF membranes and, after being blocked with 5% dry milk/0.1% Tween-20, incubated with primary antibodies in the same solution. Bound antibodies were detected by anti-rabbit or -mouse IgG conjugated with peroxidase and subsequent chemiluminescent detection.

IRS-1 serine phosphorylation. Homogenate (1 mg protein) was incubated with a rabbit anti–IRS-1 antibody bound to protein A-Sepharose to immunoprecipitate IRS-1, and serine phosphorylation was detected by Western blotting with an anti–phospho–IRS-1 (Ser307) antibody.

Caspase-3 activity assay. Caspase-3 activity was measured using a kit from Promega Corp. Muscle lysate was prepared from muscle samples by Dounce homogenization in lysis buffer provided with the kit. The lysates were centrifuged at 15,000 *g* for 20 minutes at 4°C, and the supernatants containing 100 μg protein were used for caspase-3 assay. Caspase-3 activity was examined by measurement of the rate of cleavage of colorimetric-conjugated substrate Ac-DEVD-pan. The specificity of the assay was confirmed by addition of the specific inhibitor DEVD-CHO in the reaction mixture at a concentration of 50 μM during the incubation.

Calpain activity assay. Calpain activity was measured using a kit from BioVision Inc. Muscle lysates were prepared from gastrocnemius muscle samples by Dounce homogenization in extraction buffer provided with the kit. The lysates were centrifuged at 10,000 g for 3 minutes at 4°C, and the supernatants containing 200 μg protein were used for calpain assay. Calpain activity was examined by measurement of the rate of cleavage of calpain substrate Ac–leucine-leucine-tyrosine–7-amino-trifluoromethyl coumarin (Ac-LLY-AFC). Free AFC emits a yellow-green fluorescence, which was detected using a fluorometer (Synergy HT; Bio-Tek Instruments Inc.) equipped with a 400-nm excitation filter and a 505-nm emission filter. Calpain activity was expressed as relative fluorescence units per milligram protein of each sample.

Actin cleavage. Gastrocnemius muscles were homogenized in hypotonic buffer composed of 5 mM Tris-HCl (pH 8.0), 1 mM EDTA, 1 mM EGTA, 1 mM β-mercaptoethanol, 1% glycerol with 0.1 mM PMSF, leupeptin (5 μg/ml), and aprotinin (5 μg/ml). The homogenates were centrifuged (1,600 *g* for 10 minutes), the pellet was resuspended in the hypotonic buffer, and the prepared extracts were incubated at 37°C for 2 hours with or without the caspase-3 inhibitor DEVD-CHO (50 μM). Equal volumes of Laemmli sample buffer were then added for SDS-PAGE and Western blot analysis using C-terminus–specific anti-actin antibody.

Real-time PCR. RNA was extracted using the RNeasy kit (QIAGEN Inc.), and cDNA was synthesized using the first-strand cDNA synthesis kit with random primers (Amersham Biosciences). Real-time PCR was performed using the iCycler (Bio-Rad Laboratories) with the following primers: for mouse IGF-1, 5′-TGCTCTTCAGTTCGTGTG, 5′-ACATCTCCAGTCTCCTCAG: for mouse atrogin-1, 5′-GCAGAGAGTCGGCAAGTC, 5′-CAGGTCGGTGATCGTGAG; or for mouse MuRF-1, 5′-CAACCTGTGCCGCAAGTG, 5′-CAACCTCGTGCCTACAAGATG. We used a 2-step amplification protocol with an annealing temperature of 53.2°C (IGF-1), 53.8°C (atrogin-1), or 55.1°C (MuRF-1) for 40 cycles. Relative expression was calculated from cycle threshold (Ct; relative expression = $2^{-(\Delta Ct - CACt)}$) values using β actin as internal control for each samples.

Potassium measurement. Plasma K^+ concentrations were analyzed by ion-specific electrodes (LX20; Beckman Coulter Inc.). Skeletal muscle K^+ content was measured as described by Bundgaard and Kjeldsen (60). Briefly, 25 mg gastrocnemius muscle samples were dissolved in 1 ml 30% H_2O_2, incubated at 90°C for 12 hours, and resuspended in 2 ml trichloroacetic acid (5% wt/vol), and 0.5 ml sample was brought to 2 ml with H_2O and K^+ measured by atomic emission (SpectrAA-400; Varian Inc.), with the help of T. Sandreczki (University of Missouri, Kansas City, Missouri, USA).

Cytochrome c assay. Gastrocnemius muscle was homogenized in isolation buffer (250 mM sucrose, 0.1 mM EGTA, 10 mM Tris-HCl, pH 7.4, and 1 tablet per 50 ml of the broad-spectrum Complete inhibitor cocktail [Roche Diagnostics]). The cytosolic fraction was obtained by centrifuging the solution at 100,000 *g* for 60 minutes. The cytosolic level of cytochrome *c* was determined by ELISA (R&D Systems) following the manufacturer's instruction. Briefly, the cytosolic fractions prepared from muscle were assayed using enzyme-linked anti–cytochrome *c* monoclonal antibody and substrate solution containing tetramethylbenzidine and hydrogen peroxide. Absorbance was measured at 450/570 nm dual wavelengths. The data were expressed as the mean optical density of the samples normalized to a percentage of the control value.

Cell death ELISA. DNA ladder assay was performed as described previously (48). In brief, 10 muscle cryosections, 20 μm thick, were solubilized in 200 μl of lysis buffer (0.1% Triton X-100, 5 mM Tris-HCl [pH 8.0], 20 mM EGTA, 20 mM EDTA). Then, polyethylene glycol 8000 and NaCl were added to final concentrations of 2.5% and 1 M, respectively. Samples were centrifuged at 16,000 *g* for 10 minutes at 4°C. Protein concentration of supernatant was determined by the method of Bradford and adjusted to 0.01 μg/μl. Cell death ELISA analysis was performed according to the manufacturer's instructions (Boehringer Mannheim). After incubation, the plates were analyzed with a multiwell plate reader.

In situ DNA nick-end labeling. In situ nick-end labeling (TUNEL) of fragmented DNA was performed on cryosections of gastrocnemius muscle (In Situ Cell Death Detection Kit; Roche Applied Science). The percentage of positive apoptotic myocytes was calculated after counting 300 myocytes using 5 different sections. Apoptotic cell index was presented as the number of TUNEL-positive cells (stained with FITC) per 100 total myocytes (stained with DAPI).

Statistical analysis. All data represent the mean ± SEM of at least 5 animals in each group, and results were analyzed using Student's *t* test when data from 2 experimental groups were compared or ANOVA when data from 3 groups were studied. For data analyzed by ANOVA, pairwise comparisons were made using Tukey's *t* test; $P < 0.05$ was considered statistically significant. All Western blotting was performed using a minimum of 3–4 pairs of samples.

Acknowledgments

This study was supported by NHLBI grant 70241 (to P. Delafontaine).

Received for publication June 2, 2004, and accepted in revised form November 16, 2004.

Address correspondence to: Patrick Delafontaine, Tulane University School of Medicine, Department of Medicine, Section of Cardiology, 1430 Tulane Avenue, SL-48, New Orleans, Louisiana 70112-2699, USA. Phone: (504) 587-2025; Fax: (504) 587-4237; E-mail: pdelafon@tulane.edu.

1. Levenson, J.W., Skerrett, P.J., and Gaziano, J.M. 2002. Reducing the global burden of cardiovascular disease: the role of risk factors. *Prev. Cardiol.* **5**:188–199.
2. Kuroda, T., and Shida, H. 1983. Angiotensin II-induced myocardial damage with a special reference to low cardiac output syndrome. *Jpn. Heart J.* **24**:235–243.
3. Anker, S.D., et al. 1997. Wasting as independent risk factor for mortality in chronic heart failure. *Lancet.* **349**:1050–1053.
4. Anker, S.D., and Rauchhaus, M. 1999. Insights into the pathogenesis of chronic heart failure: immune activation and cachexia. *Curr. Opin. Cardiol.* **14**:211–216.
5. Brink, M., Wellen, J., and Delafontaine, P. 1996. Angiotensin II causes weight loss and decreases circulating insulin-like growth factor I in rats through a pressor-independent mechanism. *J. Clin. Invest.* **97**:2509–2516.
6. Sandri, M., et al. 2004. Foxo transcription factors induce the atrophy-related ubiquitin ligase atrogin-1 and cause skeletal muscle atrophy. *Cell.* **117**:399–412.
7. Lecker, S.H., et al. 2004. Multiple types of skeletal muscle atrophy involve a common program of changes in gene expression. *FASEB J.* **18**:39–51.
8. Vescovo, G., et al. 2000. Apoptosis in the skeletal muscle of patients with heart failure: investigation of clinical and biochemical changes. *Heart.* **84**:431–437.
9. Agusti, A.G., et al. 2002. Skeletal muscle apoptosis and weight loss in chronic obstructive pulmonary disease. *Am. J. Respir. Crit. Care Med.* **166**:485–489.
10. Du, J., et al. 2004. Activation of caspase-3 is an initial step triggering accelerated muscle proteolysis in catabolic conditions. *J. Clin. Invest.* **113**:115–123. doi:10.1172/JCI200418330.
11. Bark, T.H., McNurlan, M.A., Lang, C.H., and Garlick, P.J. 1998. Increased protein synthesis after

acute IGF-I or insulin infusion is localized to muscle in mice. *Am. J. Physiol.* **275**:E118–E123.
12. Barton, E.R., Morris, L., Musaro, A., Rosenthal, N., and Sweeney, H.L. 2002. Muscle-specific expression of insulin-like growth factor I counters muscle decline in mdx mice. *J. Cell Biol.* **157**:137–148.
13. Bodine, S.C., et al. 2001. Identification of ubiquitin ligases required for skeletal muscle atrophy. *Science.* **294**:1704–1708.
14. Goll, D.E., Thompson, V.F., Li, H., Wei, W., and Cong, J. 2003. The calpain system. *Physiol. Rev.* **83**:731–801.
15. Tidball, J.G., and Spencer, M.J. 2002. Expression of a calpastatin transgene slows muscle wasting and obviates changes in myosin isoform expression during murine muscle disuse. *J. Physiol.* **545**:819–828.
16. Neumar, R.W., Xu, Y.A., Gada, H., Guttmann, R.P., and Siman, R. 2003. Cross-talk between calpain and caspase proteolytic systems during neuronal apoptosis. *J. Biol. Chem.* **278**:14162–14167.
17. Suhara, T., Kim, H.S., Kirshenbaum, L.A., and Walsh, K. 2002. Suppression of Akt signaling induces Fas ligand expression: involvement of caspase and Jun kinase activation in Akt-mediated Fas ligand regulation. *Mol. Cell. Biol.* **22**:680–691.
18. Folli, F., Kahn, C.R., Hansen, H., Bouchie, J.L., and Feener, E.P. 1997. Angiotensin II inhibits insulin signaling in aortic smooth muscle cells at multiple levels. A potential role for serine phosphorylation in insulin/angiotensin II crosstalk. *J. Clin. Invest.* **100**:2158–2169.
19. Velloso, L.A., et al. 1996. Cross-talk between the insulin and angiotensin signaling systems. *Proc. Natl. Acad. Sci. U. S. A.* **93**:12490–12495.
20. Motley, E.D., et al. 2003. Insulin-induced Akt activation is inhibited by angiotensin II in the vasculature through protein kinase C-alpha. *Hypertension.* **41**:775–780.
21. Tseng, Y.H., Ueki, K., Kriauciunas, K.M., and Kahn, C.R. 2002. Differential roles of insulin receptor substrates in the anti-apoptotic function of insulin-like growth factor-1 and insulin. *J. Biol. Chem.* **277**:31601–31611.
22. Chandrashekhar, Y., Sen, S., Anway, R., Shuros, A., and Anand, I. 2004. Long-term caspase inhibition ameliorates apoptosis, reduces myocardial troponin-I cleavage, protects left ventricular function, and attenuates remodeling in rats with myocardial infarction. *J. Am. Coll. Cardiol.* **43**:295–301.
23. Grady, E.F., Sechi, L.A., Griffin, C.A., Schambelan, M., and Kalinyak, J.E. 1991. Expression of AT2 receptors in the developing rat fetus. *J. Clin. Invest.* **88**:921–933.
24. Tsutsumi, K., Stromberg, C., Viswanathan, M., and Saavedra, J.M. 1991. Angiotensin-II receptor subtypes in fetal tissue of the rat: autoradiography, guanine nucleotide sensitivity, and association with phosphoinositide hydrolysis. *Endocrinology.* **129**:1075–1082.
25. Brink, M., et al. 2001. Angiotensin II induces skeletal muscle wasting through enhanced protein degradation and down-regulates autocrine insulin-like growth factor I. *Endocrinology.* **142**:1489–1496.
26. Auclair, D., Garrel, D.R., Chaouki Zerouala, A., and Ferland, L.H. 1997. Activation of the ubiquitin pathway in rat skeletal muscle by catabolic doses of glucocorticoids. *Am. J. Physiol.* **272**:C1007–C1016.
27. Gayan-Ramirez, G., Vanderhoydonc, F., Verhoeven, G., and Decramer, M. 1999. Acute treatment with corticosteroids decreases IGF-1 and IGF-2 expression in the rat diaphragm and gastrocnemius. *Am. J. Respir. Crit. Care Med.* **159**:283–289.
28. May, R.C., Kelly, R.A., and Mitch, W.E. 1986. Metabolic acidosis stimulates protein degradation in rat muscle by a glucocorticoid-dependent mechanism. *J. Clin. Invest.* **77**:614–621.
29. Mitch, W.E., et al. 1999. Evaluation of signals activating ubiquitin-proteasome proteolysis in a model of muscle wasting. *Am. J. Physiol.* **276**:C1132–C1138.
30. Price, S.R., England, B.K., Bailey, J.L., Van Vreede, K., and Mitch, W.E. 1994. Acidosis and glucocorticoids concomitantly increase ubiquitin and proteasome subunit mRNAs in rat muscle. *Am. J. Physiol.* **267**:C955–C960.
31. Youssef, J.A., and Badr, M.Z. 2003. Hepatocarcinogenic potential of the glucocorticoid antagonist RU486 in B6C3F1 mice: effect on apoptosis, expression of oncogenes and the tumor suppressor gene p53. *Mol. Cancer.* **2**:3.
32. Musaro, A., et al. 2001. Localized Igf-1 transgene expression sustains hypertrophy and regeneration in senescent skeletal muscle. *Nat. Genet.* **27**:195–200.
33. Datta, S.R., et al. 1997. Akt phosphorylation of BAD couples survival signals to the cell-intrinsic death machinery. *Cell.* **91**:231–241.
34. del Peso, L., Gonzalez-Garcia, M., Page, C., Herrera, R., and Nunez, G. 1997. Interleukin-3-induced phosphorylation of BAD through the protein kinase Akt. *Science.* **278**:687–689.
35. Sjogren, K., et al. 1999. Liver-derived insulin-like growth factor I (IGF-I) is the principal source of IGF-I in blood but is not required for postnatal body growth in mice. *Proc. Natl. Acad. Sci. U. S. A.* **96**:7088–7092.
36. Yakar, S., et al. 1999. Normal growth and development in the absence of hepatic insulin-like growth factor I. *Proc. Natl. Acad. Sci. U. S. A.* **96**:7324–7329.
37. Wing, S.S., and Goldberg, A.L. 1993. Glucocorticoids activate the ATP-ubiquitin-dependent proteolytic system in skeletal muscle during fasting. *Am. J. Physiol.* **264**:E668–E676.
38. May, R.C., Bailey, J.L., Mitch, W.E., Masud, T., and England, B.K. 1996. Glucocorticoids and acidosis stimulate protein and amino acid catabolism in vivo. *Kidney Int.* **49**:679–683.
39. Musaro, A., and Rosenthal, N. 1999. Maturation of the myogenic program is induced by postmitotic expression of insulin-like growth factor I. *Mol. Cell. Biol.* **19**:3115–3124.
40. Fryburg, D.A., Jahn, L.A., Hill, S.A., Oliveras, D.M., and Barrett, E.J. 1995. Insulin and insulin-like growth factor-I enhance human skeletal muscle protein anabolism during hyperaminoacidemia by different mechanisms. *J. Clin. Invest.* **96**:1722–1729.
41. DeVol, D.L., Rotwein, P., Sadow, J.L., Novakofski, J., and Bechtel, P.J. 1990. Activation of insulin-like growth factor gene expression during work-induced skeletal muscle growth. *Am. J. Physiol.* **259**:E89–E95.
42. Rommel, C., et al. 2001. Mediation of IGF-1-induced skeletal myotube hypertrophy by PI(3)K/Akt/mTOR and PI(3)K/Akt/GSK3 pathways. *Nat. Cell Biol.* **3**:1009–1013.
43. Glass, D.J. 2003. Signalling pathways that mediate skeletal muscle hypertrophy and atrophy. *Nat. Cell Biol.* **5**:87–90.
44. Duncan, A.M., Burrell, L.M., Kladis, A., and Campbell, D.J. 1997. Angiotensin and bradykinin peptides in rats with myocardial infarction. *J. Card. Fail.* **3**:41–52.
45. Nave, B.T., Ouwens, M., Withers, D.J., Alessi, D.R., and Shepherd, P.R. 1999. Mammalian target of rapamycin is a direct target for protein kinase B: identification of a convergence point for opposing effects of insulin and amino-acid deficiency on protein translation. *Biochem. J.* **344**:427–431.
46. Beugnet, A., Tee, A.R., Taylor, P.M., and Proud, C.G. 2003. Regulation of targets of mTOR (mammalian target of rapamycin) signalling by intracellular amino acid availability. *Biochem. J.* **372**:555–566.
47. Liu, Z., Jahn, L.A., Wei, L., Long, W., and Barrett, E.J. 2002. Amino acids stimulate translation initiation and protein synthesis through an Akt-independent pathway in human skeletal muscle. *J. Clin. Endocrinol. Metab.* **87**:5553–5558.
48. Vescovo, G., et al. 2002. L-Carnitine: a potential treatment for blocking apoptosis and preventing skeletal muscle myopathy in heart failure. *Am. J. Physiol., Cell Physiol.* **283**:C802–C810.
49. Adams, V., et al. 1999. Apoptosis in skeletal myocytes of patients with chronic heart failure is associated with exercise intolerance. *J. Am. Coll. Cardiol.* **33**:959–965.
50. Hambrecht, R., et al. 2002. Reduction of insulin-like growth factor-I expression in the skeletal muscle of noncachectic patients with chronic heart failure. *J. Am. Coll. Cardiol.* **39**:1175–1181.
51. Anker, S.D., et al. 1997. Tumor necrosis factor and steroid metabolism in chronic heart failure: possible relation to muscle wasting. *J. Am. Coll. Cardiol.* **30**:997–1001.
52. Pedersen, E.B., et al. 1986. Angiotensin II, aldosterone and arginine vasopressin in plasma in congestive heart failure. *Eur. J. Clin. Invest.* **16**:56–60.
53. Staroukine, M., Devriendt, J., Decoodt, P., and Verniory, A. 1984. Relationships between plasma epinephrine, norepinephrine, dopamine and angiotensin II concentrations, renin activity, hemodynamic state and prognosis in acute heart failure. *Acta Cardiol.* **39**:131–138.
54. Ladner, K.J., Caligiuri, M.A., and Guttridge, D.C. 2003. Tumor necrosis factor-regulated biphasic activation of NF-kappa B is required for cytokine-induced loss of skeletal muscle gene products. *J. Biol. Chem.* **278**:2294–2303.
55. Reid, M.B., Lannergren, J., and Westerblad, H. 2002. Respiratory and limb muscle weakness induced by tumor necrosis factor-alpha: involvement of muscle myofilaments. *Am. J. Respir. Crit. Care Med.* **166**:479–484.
56. Anker, S.D., et al. 1999. Cytokines and neurohormones relating to body composition alterations in the wasting syndrome of chronic heart failure. *Eur. Heart J.* **20**:683–693.
57. Anker, S.D., et al. 1997. Hormonal changes and catabolic/anabolic imbalance in chronic heart failure and their importance for cardiac cachexia. *Circulation.* **96**:526–534.
58. Kasahara, Y., et al. 2000. Inhibition of VEGF receptors causes lung cell apoptosis and emphysema. *J. Clin. Invest.* **106**:1311–1319.
59. Davani, S., et al. 2003. Mesenchymal progenitor cells differentiate into an endothelial phenotype, enhance vascular density, and improve heart function in a rat cellular cardiomyoplasty model. *Circulation.* **108**(Suppl 1):II253–II258.
60. Bundgaard, H., and Kjeldsen, K. 2002. Potassium depletion increases potassium clearance capacity in skeletal muscles in vivo during acute repletion. *Am. J. Physiol., Cell Physiol.* **283**:C1163–C1170.